

# Shape optimization of elastic structures using a level-set based mesh evolution method

Grégoire Allaire<sup>1</sup>, Charles Dapogny<sup>2,3</sup> and Pascal Frey<sup>2</sup>

<sup>1</sup> Centre de Mathématiques Appliquées (UMR 7641), Ecole Polytechnique, Palaiseau, France

<sup>2</sup> UPMC Univ Paris 06, UMR 7598, Laboratoire J.L. Lions, Paris, France

<sup>3</sup> RENAULT, Direction de la recherche et des études avancées, 78280 Guyancourt, France

e-mails: [gregoire.allaire@polytechnique.fr](mailto:gregoire.allaire@polytechnique.fr), [{dapogny,frey}@ann.jussieu.fr](mailto:{dapogny,frey}@ann.jussieu.fr)

## Abstract

We propose a method for structural optimization that combines two different ways of depicting shapes : the considered domain is exactly meshed at each iteration when it comes to performing shape or topological sensitivity analysis of the considered cost functional (which often requires one or several finite element computations), while we resort to a level-set description of the domain for describing its evolution along the derived gradient velocity field. The cornerstone of this method is a meshing algorithm for building a mesh, suitable for mechanical computations, out of a piecewise linear level-set function on an unstructured mesh. The proposed method thus enjoys an accurate description of the shapes at hand, and still allows for topological changes thanks to the versatility of level-set methods.

## 1 Introduction

Since the seminal papers [2] [3] and [20], the level-set method of Osher and Sethian [14] has proved to be a very versatile tool in the context of structural optimization. Working on a large computational domain  $\mathcal{D} \subset \mathbb{R}^d$ , endowed with a fixed Cartesian grid, the authors used a consistent approximation of the mechanical problem at stake - namely the *ersatz material approach* - then applied classical shape sensitivity techniques (the so-called Hadamard method [1], [13], [18]) and described the evolution of the shape  $\Omega \subset \mathcal{D}$  by a Hamilton-Jacobi equation for the associated level-set function. Here, we propose a new approach where the shape  $\Omega$  is exactly meshed at each iteration and no ersatz material is necessary in the void region  $\mathcal{D} \setminus \Omega$ . We still rely on a larger computational domain  $\mathcal{D}$  which is no longer meshed with a fixed Cartesian grid, but rather is endowed with an *unstructured* mesh that is notably changed at each iteration of the optimization process (using local mesh modification/adaptation techniques [9]) so that the shape  $\Omega$  is precisely captured, i.e. its boundary is a collection of internal edges (in  $2d$ ) or faces (in  $3d$ ) of the mesh. The level-set method is still a key ingredient for mesh deformation and, as such, allows for topology changes from one iteration to the next. However, this approach rises several technical points : we are inherently working on unstructured meshes, and thus can no longer rely on classical numerical schemes for the 'standard' level set operations : distancing/redistancing algorithm, method for solving the Hamilton-Jacobi equation,...

This paper is organized as follows. Section 2 introduces the linear elasticity model that will be at stake in the following, and sets some notations. Then, section 3 describes the two different standpoints from which shapes will be considered, as well as their relationship. Section 4 is meant to recall the sensitivity analysis tools which allow to infer descent velocity fields for the considered objective functionals, and section 5 briefly explains how the evolution of the shape is described in the level-set context. Eventually, section 6 sums up the various steps of the proposed method, and some examples are provided in section 8.

We emphasize that, whilst all our numerical examples here are presented in the  $2d$  setting, the whole method has been devised with the  $3d$  case in mind : no subsequent theoretical difficulty should arise in this context.

## 2 A model problem in linear elasticity

In this paper, we are interested in the optimization of a *shape*  $\Omega$ , that is, a bounded domain of  $\mathbb{R}^d$ , made of a linear isotropic material, subjected to Hooke's law  $A$ . Such a shape is clamped on a part  $\Gamma_D$  of its boundary  $\partial\Omega$ , and submitted to surface loads  $g \in H^2(\mathbb{R}^d)^d$  on the complementary part  $\Gamma_N = \partial\Omega \setminus \Gamma_D$ , with  $\Gamma_D$  and  $\Gamma_N$  being of positive  $(d-1)$ -measure in  $\partial\Omega$ . For the sake of simplicity, we neglect body forces and restrict ourselves to linearized elasticity. In this context, the displacement field  $u = u_\Omega$  of the shape is the unique solution in  $H^1(\Omega)^d$  of the *linear elasticity system*

$$\begin{cases} -\operatorname{div}(Ae(u)) &= 0 & \text{in } \Omega, \\ u &= 0 & \text{on } \Gamma_D, \\ Ae(u) \cdot n &= g & \text{on } \Gamma_N, \end{cases} \quad (1)$$

where  $e(u) = \frac{1}{2}((\nabla u)^t + \nabla u)$  is the *strain tensor* and  $n$  is the outer unit normal to  $\partial\Omega$ . We aim at finding a shape  $\Omega$  that minimizes a given objective function  $J(\Omega)$  among a set  $\mathcal{U}_{ad}$  of *admissible shapes* which may involve geometric constraints such as  $\Omega \subset \mathcal{D}$  and a fixed total volume  $V(\Omega)$ . Common interesting choices of such functional are the *compliance*  $J_1(\Omega)$  of structure  $\Omega$ , or a least-square discrepancy criterion  $J_2(\Omega)$  between the displacement field  $u_\Omega$  and a target displacement  $u_0 \in H^1(\mathbb{R}^d)^d$  (with a weight coefficient  $k(x)$ ), for  $\alpha \geq 2$ :

$$J_1(\Omega) = \int_{\Gamma_N} g \cdot u_\Omega \, ds \quad ; \quad J_2(\Omega) = \left( \int_{\Omega} k |u_\Omega - u_0|^\alpha \, dx \right)^{\frac{1}{\alpha}}. \quad (2)$$

In all our examples, a constraint on the total volume of the structure is added and incorporated by a simple penalization method, with a fixed positive Lagrange multiplier  $\ell$ , so that the optimization problem becomes

$$\inf_{\Omega \subset \mathcal{D}} \left( J(\Omega) + \ell V(\Omega) \right). \quad (3)$$

As explained in [3], there are no difficulties to extend our approach to more general objective functions, to additional constraints and to non-linear elasticity.

## 3 Two complementary ways for representing shapes

We alternatively represent a shape  $\Omega \subset \mathcal{D}$  as a mesh  $\mathcal{T}_\Omega$  of the *whole* computational domain  $\mathcal{D}$  in which  $\Omega$  is *explicitly* discretized (so that a mesh of  $\Omega$  is included in  $\mathcal{T}_\Omega$  as a submesh - see figure 1) and as a level-set function  $\psi_\Omega$ , defined on  $\mathcal{D}$  (in numerical practice it is a  $\mathbb{P}^1$ -Lagrange finite element function on an unstructured mesh), enjoying the properties

$$\Omega = \{x \in \mathcal{D} \mid \psi_\Omega(x) < 0\} \quad ; \quad \partial\Omega = \{x \in \mathcal{D} \mid \psi_\Omega(x) = 0\}. \quad (4)$$

Both representations are used at different steps of our method: thus, a crucial ingredient is an efficient tool for switching from one characterization to the other.

### 3.1 Generating a level-set function associated to a shape

Let  $\Omega \subset \mathcal{D}$  be a subdomain, explicitly discretized in the mesh  $\mathcal{T}$  of  $\mathcal{D}$  (even though the method straightforwardly extends to the case of a non-discretized interface). It is classical to generate a corresponding level-set function by computing the signed distance function to  $\Omega$ , at least near the interface  $\partial\Omega$  [6]. To this end, we use a numerical scheme for unstructured (simplicial) meshes, based on some properties of the unique viscosity solution of the time-dependent Eikonal equation, which is described in detail in a previous work [7] (see e.g. [16] for an alternative).

### 3.2 Meshing the negative subdomain of a level set function, ensuring conformity with the positive subdomain

Given an initial triangular mesh  $\mathcal{T}$  of  $\mathcal{D}$ , the 0 level-set of a  $\mathbb{P}^1$  finite element function  $\psi$  is a piecewise affine curve (surface in 3d). To obtain a (new) mesh of the shape  $\Omega$ , corresponding to  $\psi$  through (4), we proceed in two, or three, steps (see figure1) :

1. Each simplex  $K \in \mathcal{T}$ , crossed by the 0 level-set of function  $\psi$  is split in such a way that  $K \cap \partial\Omega$  belongs to the resulting mesh  $\tilde{\mathcal{T}}$ , which has to remain conformal. To this end, a pattern which enumerates the various possible configurations is used [9]. Unfortunately, the intersections of  $\partial\Omega$  with the mesh  $\mathcal{T}$  are not controlled at this stage and the resulting mesh  $\tilde{\mathcal{T}}$  is bound to be of very poor quality as far as finite element computations are concerned (ill-shaped elements, e.g. very flat or small, are likely to appear).
2. A local mesh improvement is performed, so that a new improved quality mesh  $\mathcal{T}'$  is created. This step relies on local mesh modification operators (collapse of close points, points relocations,...) described in [9].
3. (Optional) The mesh  $\mathcal{T}'$  is smoothed, especially near the boundary  $\partial\Omega$ , with a mesh regularization procedure [9] to remove small angles or bumps on  $\partial\Omega$  that could impair the accuracy of the finite element computations to come.

## 4 Shape and topological sensitivity analysis

### 4.1 Shape sensitivity analysis

This is the so-called *Hadamard's method*, which has been described on the theoretical side in [13] (see also [18] [12]) and successfully used in [3] in the context of level-set methods.

Given a reference bounded domain  $\Omega_0$ , for  $\theta \in W^{1,\infty}(\mathbb{R}^d, \mathbb{R}^d)$  small enough,  $(I + \theta)$  is a Lipschitz diffeomorphism of  $\mathbb{R}^d$ , with Lipschitz inverse and we consider variations of the form  $\Theta_{ad} \ni \theta \mapsto (I + \theta)\Omega_0 \in \mathbb{R}^d$ , where  $\Theta_{ad}$  is a subset of  $W^{1,\infty}(\mathbb{R}^d, \mathbb{R}^d)$  corresponding to *admissible* variations of the shape (see [3] again). An objective function  $J(\Omega)$  is said to be *shape-differentiable* at  $\Omega_0$  if the application  $\theta \mapsto J((I + \theta)\Omega_0)$  is Fréchet-differentiable at 0 and the associated Fréchet differential  $dJ(\Omega_0)(\theta)$  is the *shape derivative* of  $J$  at  $\Omega_0$ . The following theorem accounts for the shape differentiability of the objective functions  $J_1$  and  $J_2$  of interest (see [3] for considerations in a more general case) :

**Theorem 4.1**  $\Omega \subset \mathbb{R}^d$  being a smooth bounded domain, the compliance  $J_1$  as well as the least-square criterion  $J_2$  are shape-differentiable at  $\Omega$ , with shape derivatives

$$\forall \theta \in \Theta_{ad}, \quad dJ_1(\Omega)(\theta) = \int_{\Gamma_N} \left( 2 \left( \frac{\partial(g \cdot u_\Omega)}{\partial n} + \kappa g \cdot u_\Omega \right) - Ae(u_\Omega) : e(u_\Omega) \right) \theta \cdot n \, ds + \int_{\Gamma_D} Ae(u_\Omega) : e(u_\Omega) \theta \cdot n \, ds, \quad (5)$$

$$\forall \theta \in \Theta_{ad}, \quad dJ_2(\Omega)(\theta) = \int_{\Gamma_N} \left( \frac{C_0}{\alpha} k |u - u_0|^\alpha + Ae(u_\Omega) : e(p_\Omega) - \frac{\partial(g \cdot p_\Omega)}{\partial n} - \kappa g \cdot p_\Omega \right) \theta \cdot n \, ds + \int_{\Gamma_D} \left( \frac{C_0}{\alpha} k |u - u_0|^\alpha - Ae(u_\Omega) : e(p_\Omega) \right) \theta \cdot n \, ds, \quad (6)$$

where  $\kappa$  is the mean curvature of  $\partial\Omega$ ,  $C_0 = \left( \int_{\Omega} k|u - u_0|^\alpha dx \right)^{\frac{1}{\alpha-1}}$  is a constant, and  $p_\Omega \in H^1(\Omega)^d$  is the adjoint state to the system, unique solution to the system :

$$\begin{cases} -\operatorname{div}(Ae(p)) &= -C_0 k|u - u_0|^{\alpha-2}(u - u_0) & \text{in } \Omega, \\ p &= 0 & \text{on } \Gamma_D, \\ Ae(p) \cdot n &= 0 & \text{on } \Gamma_N, \end{cases} \quad (7)$$

Theorem 4.1 yields a velocity field, *a priori* defined on the boundary  $\partial\Omega$ , according to which this boundary has to be deformed so as to decrease the objective function under consideration.

Note that this velocity field is relevant only on the boundary  $\partial\Omega$ , while it should be defined on the whole computational domain because the deformation is accounted for by level set methods. It has then to be extended to this domain, and several consistant methods are available to achieve this. See [5] [11] for a complete discussion over this topic.

## 4.2 Topological sensitivity analysis

The previous method produces a deformation of the boundary  $\partial\Omega$  that allows a decrease of  $J(\Omega)$ , and in particular forbids topological changes (at least theoretically), making the resulting shape strongly dependent on the initialization of the algorithm. As highlighted by [4] or [10], the coupling with a mechanism that evaluates the benefit of the formation of a small hole in the structure partially overcomes this drawback.

Given a domain  $\Omega$ , an objective function  $J$  is said to admit a *topological derivative*  $D_T J(x_0)$  at  $x_0 \in \Omega$  if, for  $\rho > 0$  sufficiently small, there exists a function  $f(\rho) \rightarrow 0$  as  $\rho \rightarrow 0$ , such that the following asymptotic expansion holds :

$$J(\Omega \setminus \overline{(x_0 + \rho\omega)}) = J(\Omega) + f(\rho) D_T J(x_0) + o(\rho), \quad (8)$$

where  $\omega$  is the unit ball of  $\mathbb{R}^d$  and  $\lim_{\rho \rightarrow 0} \frac{o(\rho)}{\rho} = 0$ .

We then recall a topological derivability result in the case of the compliance function  $J_1$  although analogous statements hold in far more general cases [10].

**Theorem 4.2** *The compliance functional  $J_1$  admits a topological derivative at any point  $x_0 \in \Omega$  :*

$$D_T J_1(x_0) = \frac{\pi(\lambda + 2\mu)}{2\mu(\lambda + \mu)} (4\mu Ae(u_\Omega) : e(u_\Omega) + (\lambda - \mu) \operatorname{tr} Ae(u_\Omega) \operatorname{tr} e(u_\Omega)) (x_0) \quad (9)$$

where  $\lambda, \mu$  are the Lamé coefficients of the material at stake.

According to the result of Theorem 4.2, the objective functional can then be decreased by nucleating a small hole centered at points where the topological derivative is negative.

## 5 Deformation of the shape

Given a domain  $\Omega(t) \subset \mathbb{R}^d$ ,  $0 \leq t \leq T$  evolving in time according to a *normal* velocity field  $V = vn$  ( $n(t, \cdot)$  being the unit normal to  $\partial\Omega(t)$ ), an associated level-set function  $\psi(t, x)$ , i.e. such that (4) holds,

is solution to the *Hamilton-Jacobi equation* :

$$\begin{cases} \frac{\partial \psi}{\partial t}(t, x) + v(t, x)|\nabla \psi(t, x)| &= 0 & \text{on } (0, T) \times \mathbb{R}^d \\ \psi(0, x) &= \psi_0(x) & \text{on } \mathbb{R}^d \end{cases}, \quad (10)$$

where  $\psi_0$  is a level-set function associated to domain  $\Omega^0 := \Omega(0)$ .

Numerous ways to solve numerically such equations have been proposed [14], unfortunately most of them being finite difference schemes that inherently rely on a structured computational grid, whereas we need to deal with it in the unstructured context. To this end, we rely on a semi-lagrangian approach [19], which mainly consists in rewriting (10) as a standard linear advection equation

$$\begin{cases} \frac{\partial \psi}{\partial t}(t, x) + V(t, x) \cdot \nabla \psi(t, x) &= 0 & \text{on } (0, T) \times \mathbb{R}^d \\ \psi(0, x) &= \psi_0(x) & \text{on } \mathbb{R}^d \end{cases}. \quad (11)$$

The latter equation is then numerically solved by the *method of characteristics* [15] ; assuming enough regularity for the data  $\psi_0$  and  $V$ , the unique smooth solution to (11) reads : for all  $0 \leq t \leq T$  and every  $x \in \mathbb{R}^d$ ,  $\psi(t, x) = \psi_0(X(0, t, x))$ , where the *characteristic curve emerging from  $x$*   $s \mapsto X(s, t, x)$  is the unique solution to the ODE (which is numerically discretized by a 4<sup>th</sup> order Runge-Kutta method) :

$$\begin{cases} \frac{dX}{ds}(s, t, x) &= V(s, X(s, t, x)) & \text{for } s \in (0, t) \\ X(t, t, x) &= x \end{cases}. \quad (12)$$

This recasting of the problem can be interpreted as a linearly implicit scheme for the true nonlinear Hamilton-Jacobi equation.

## 6 Numerical algorithm

Starting from an initial shape  $\Omega^0$  (e.g. the full computational domain  $\mathcal{D}$ ), we get a decreasing sequence  $\Omega^k$  of shapes with respect to function  $J$  by applying a shape-sensitivity analysis (section 4) on the actual domain discretized under the form of a computational mesh, and evolve it with respect to the inferred shape derivative resorting to a level-set description (section 5). From times to times (say, every  $k_{top}$  step), we perform a topological sensitivity analysis instead of a shape sensitivity analysis so as to change the topology of the shape if need be. The proposed steepest-descent algorithm reads as follows (for clarity, we reported only the steps related to shape-sensitivity analysis, the other ones being easier) :

**For  $k \geq 0$ , until convergence**, start with a shape  $\Omega^k \subset \mathcal{D}$ , the latter being equipped with a mesh  $\mathcal{T}^k$  which encloses a mesh of  $\Omega^k$ .

1. Consider only the part related to  $\Omega^k$  in the mesh  $\mathcal{T}^k$ , and compute the solution  $u_{\Omega^k}$  to the elasticity system (1) on this submesh.
2. Generate the signed distance function  $\psi_{\Omega^k}$  associated to  $\Omega^k$ , on mesh  $\mathcal{T}^k$ .
3. Infer from (6) the vector-valued velocity field  $\theta^k$  for the advection of the shape to come.
4. Solve the following level set advection equation on the time interval  $[0, \tau^k]$  ( $\tau^k > 0$  being a descent step for the gradient algorithm)

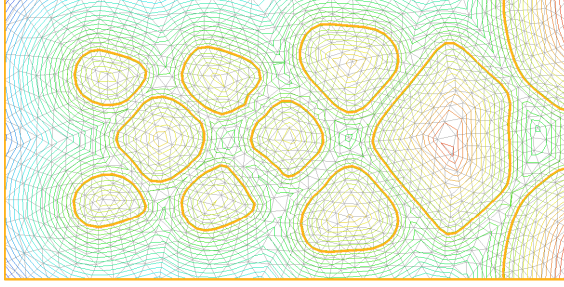
$$\begin{cases} \frac{\partial \psi}{\partial t}(t, x) + \theta^k(x) \cdot \nabla \psi(t, x) &= 0 & \text{in } (0, \tau^k) \times \mathcal{D} \\ \psi(0, x) &= \psi_{\Omega^k}(x) & \text{in } \mathcal{D} \end{cases}. \quad (13)$$

to get the level set function  $\psi(\tau^k, \cdot)$  which corresponds to the new shape  $\Omega^{k+1}$ .

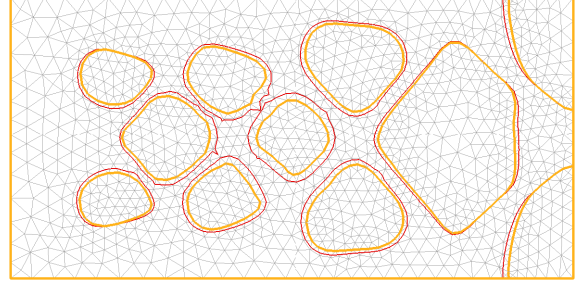
5. Discretize the 0-level set of  $\widetilde{\psi_{\Omega^{k+1}}} = \psi(\tau^k, .)$  in the mesh  $\mathcal{T}^k$  as in section 3, to get the new mesh  $\mathcal{T}^{k+1}$  of  $\mathcal{D}$ , the interior part of which yields a mesh of  $\Omega^{k+1}$ .

Note that while this algorithm is quite similar to a mesh adaptation technique, it does not require any interpolation whatsoever between two successive iterations, and consequently, no subsequent error is introduced.

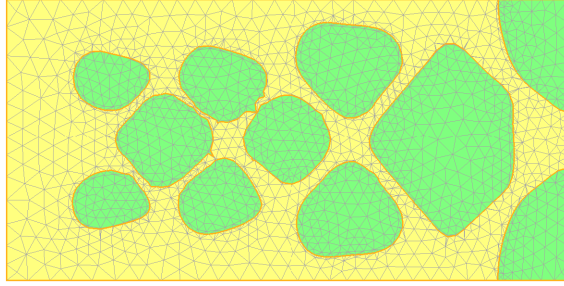
Figure 1 depicts several steps of the above algorithm.



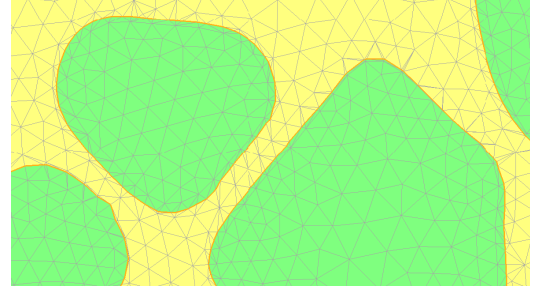
*Shape  $\Omega^k$  and some isovalues of the associated level-set function  $\psi_{\Omega^k}$ , on mesh  $\mathcal{T}^k$*



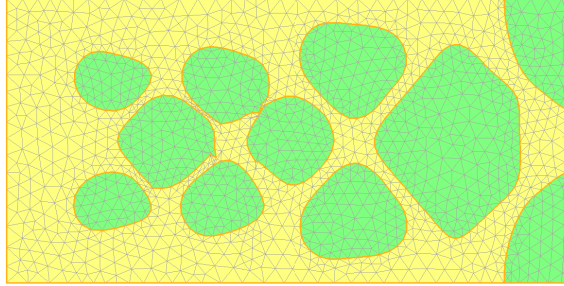
*0-level set of  $\widetilde{\psi_{\Omega^{k+1}}}$  (red line) on mesh  $\mathcal{T}^k$ .*



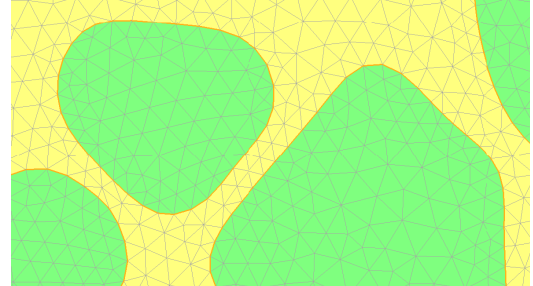
*Mesh obtained after discretization of the 0 level set of  $\widetilde{\psi_{\Omega^{k+1}}}$  in mesh  $\mathcal{T}^k$ .*



*Zoom on this mesh ; numerous ill-shaped elements are to be noted.*



*Final mesh  $\mathcal{T}^{k+1}$  after optimization.*



*Zoom on this mesh.*

Figure 1: Various steps of the proposed algorithm.

## 7 Numerical examples

All the further numerical results were obtained using an the same isotropic linear material, with normalized Young modulus  $E = 1$  and Poisson ratio  $\nu = 0.3$ . Computations are held on a MacBook Pro, with processor Intel Core Duo 2,66 Ghz, 4 Go RAM.

The first considered example is the benchmark *cantilever* test-case (see figure 2 for a description) : a cantilever lies in a  $2 \times 1$  box, is clamped on its left boundary, and submitted to a unit vertical load  $g = 1$  on a small part of its right boundary. The Lagrange multiplier is taken as  $l = 3$  and we perform

200 iterations of the algorithm described in section 6, *without* any topological derivative computation. The whole computation takes about 3 minutes and each mesh  $\mathcal{T}^k$  enjoys around 1500 vertices ( $\approx 3000$  triangles). Convergence history is reported in figure 3.

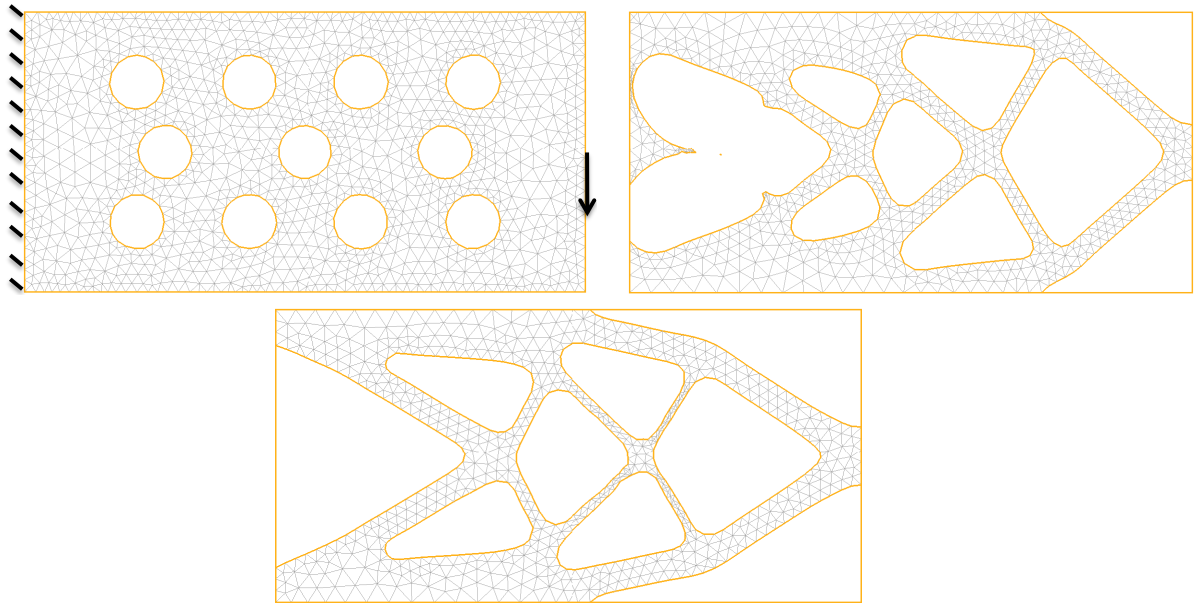


Figure 2: *Initial (top,left), intermediate (top,right) and final (bottom) iterations of the optimization of a 2d cantilever.*

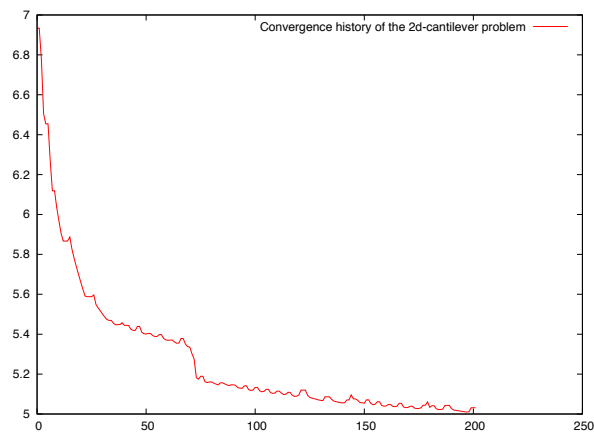


Figure 3: *Convergence history for the 2d cantilever problem.*

We then turn to another classical example, namely the so-called *optimal bridge problem* (see figure 4). Here, the computational domain is  $2 \times 1, 2$  and the Lagrange multiplier is set to 0, 1. We perform 200 iterations of the proposed algorithm, with topological derivative computation every  $k_{top} = 10$  step.

Eventually, we consider an example associated to the minimization of the least-square criterion  $J_2$  (see section 2) : a grip lying in a  $5 \times 4$  box is fixed on two small rivets, and a small force  $g$  of intensity 0.01 is applied on parts of both upper and lower boundary. The aim is to achieve a structure such that the displacement  $u_\Omega$  of the jaws of the grip is as close as possible to  $u_0 = \pm 0.5$  (see figure 5). The localizing weight factor  $k$  is chosen equal to 1 in a vicinity of the jaws of the mechanism, and to 0 elsewhere. A small volume constraint  $l = 0,001$  is added, and we perform 100 iterations of the above algorithm.



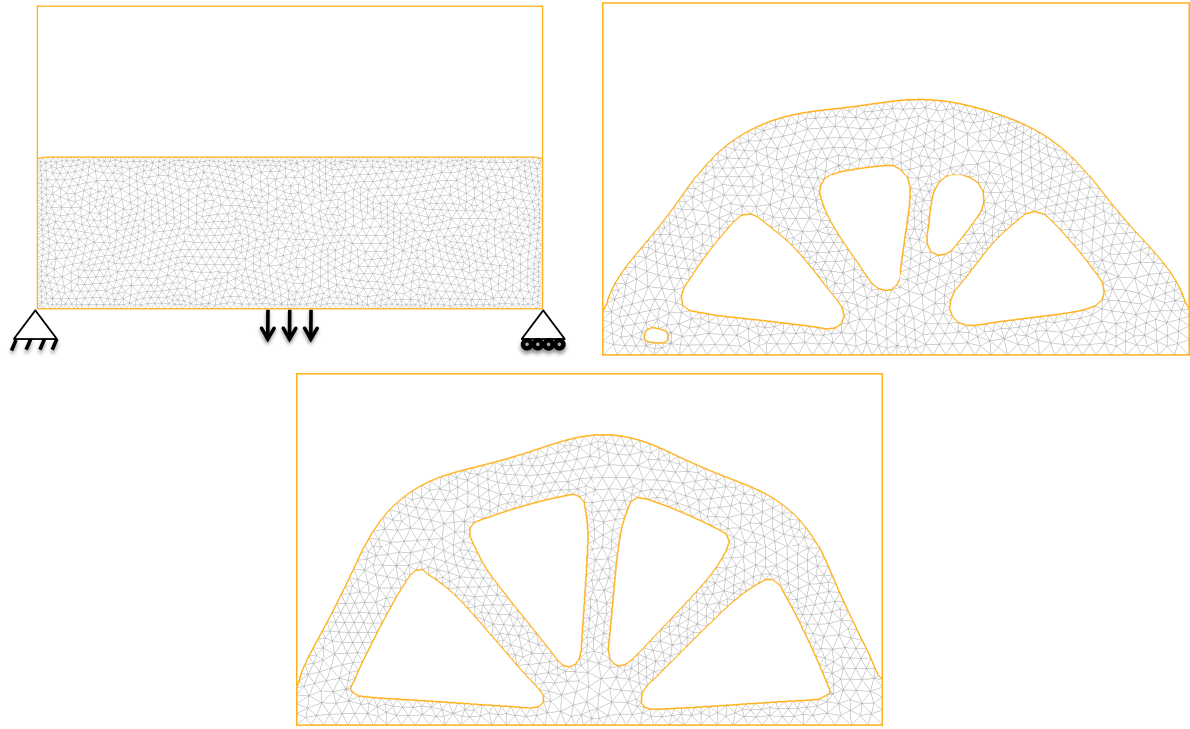


Figure 4: *Initial (top,left), intermediate (top,right) and final (bottom) iterations of the optimization of a 2d bridge.*

## 8 Conclusion and future work

We proposed a numerical method for structural optimization that combines the accuracy of a sensitivity analysis held on a well-defined domain, equipped with a computational mesh at each iteration with the versatility of level-set methods when it comes to parameterizing its evolution through the produced vector field. Several examples were presented in two space dimensions, but the method has been devised with the three-dimensional case in mind, and we believe its extension to this case should not pose any additional theoretical difficulty (even though, of course, implementation is bound to be more tedious, especially as regards meshing issues which may require additional mesh operators to be implemented). What is more, we are interested in several other objective functions, associated to various models (von Mises stress,...) ; as well, several different numerical models could be investigated with this method because the boundary of shapes is well-defined at each iteration, which is crucial, e.g. for fluid-structure interactions.

## References

- [1] G. ALLAIRE, *Conception optimale de structures*, Mathématiques & Applications, **58**, Springer Verlag, Heidelberg (2006).
- [2] G. ALLAIRE F. JOUVE A.M. TOADER, *A level-set method for shape optimization*, C. R. Acad. Sci. Paris, Série I, 334 (2002), pp.1125-1130.
- [3] G. ALLAIRE F. JOUVE A.M. TOADER, *Structural optimization using shape sensitivity analysis and a level-set method*, J. Comput. Phys., 194 (2004) pp. 363–393.
- [4] G. ALLAIRE F. DE GOURNAY F. JOUVE A.M. TOADER, *Structural optimization using topological and shape sensitivity analysis via a level-set method*, Control and Cybernetics, 34 (2005) pp. 59–80.



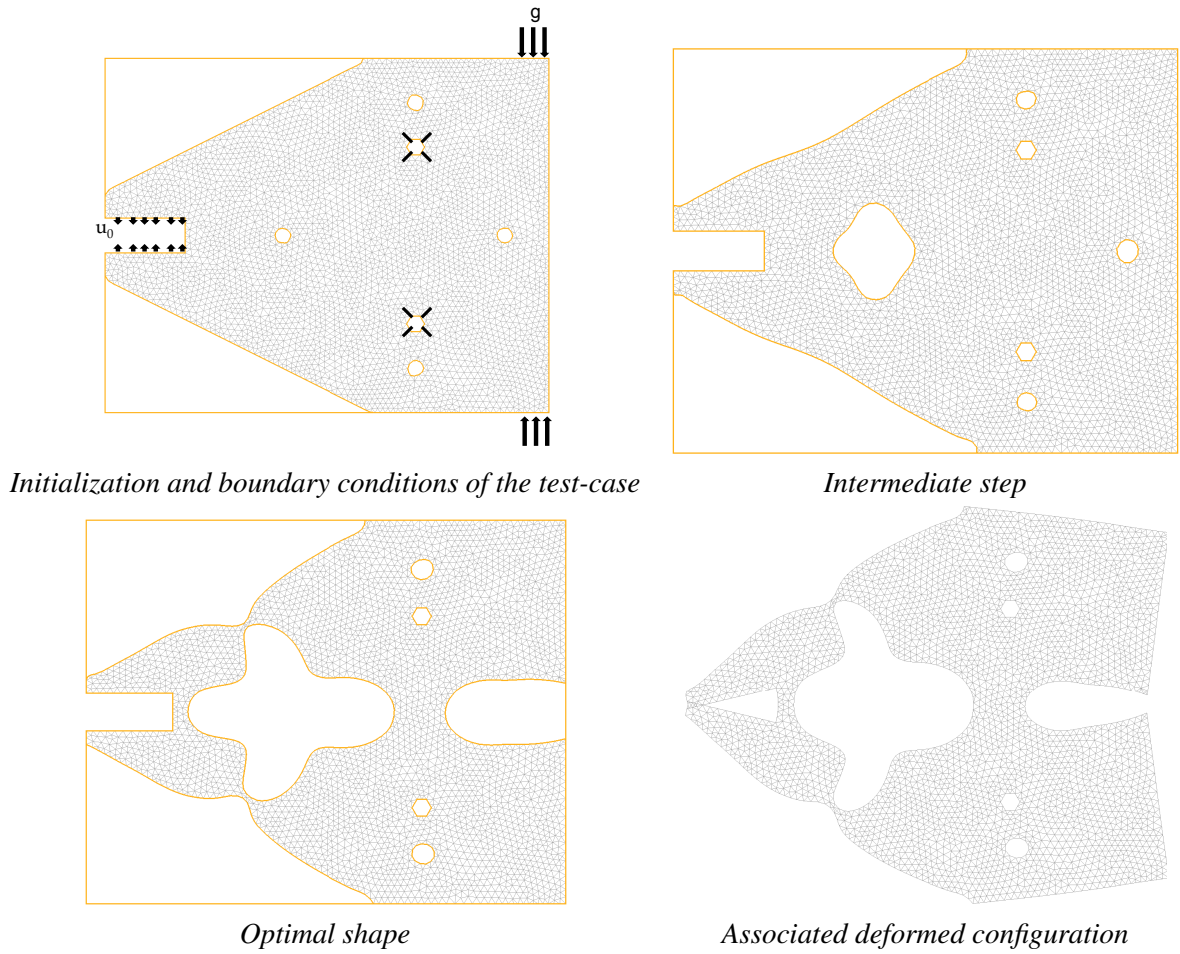


Figure 5: Optimization of a 2d gripping mechanism.

- [5] M. BURGER, *A framework for the construction of level-set methods for shape optimization and reconstruction*, Interfaces and Free Boundaries, 5 (2003) pp. 301–329.
- [6] D. CHOPP, *Computing minimal surfaces via level-set curvature flow*, J. Comput. Phys., 106 (1993), pp. 77–91.
- [7] C. DAPOGNY AND P. FREY, *Computation of the signed distance function to a discrete contour on adapted triangulation*, submitted to Calcolo (2010).
- [8] H. ESCHENAUER, V. KOBELEV, A. SCHUMACHER, *Bubble method for topology and shape optimization of structures*, Structural Optimization, **8**, 42–51 (1994).
- [9] P.J. FREY AND P.L. GEORGE, *Mesh Generation : Application to Finite Elements*, Wiley, 2nd Edition, (2008).
- [10] S. GARREAU PH. GUILLAUME M. MASMOUDI, *The topological asymptotic for PDE systems : the elasticity case*, SIAM J. Control. Optim., 39 (2001) pp. 1756–1778.
- [11] F. DE GOURNAY, *Velocity extension for the level-set method and multiple eigenvalues in shape optimization*. SIAM J. on Control and Optim., 45, no. 1, 343–367 (2006).
- [12] A. HENROT M. PIERRE, *Variation et Optimisation de Formes : une Etude Géométrique*, collection Mathématiques et Applications, vol. 48, Springer (2005).

- [13] F. MURAT J. SIMON, *Sur le contrôle par un domaine géométrique*, Technical Report RR-76015, Laboratoire d'Analyse Numérique (1976).
- [14] S.J. OSHER J.A. SETHIAN, *Fronts propagating with curvature-dependent speed : Algorithms based on Hamilton-Jacobi formulations*, J. Comput. Phys., 79 (1988), pp. 12–49.
- [15] O. PIRONNEAU, *The finite element methods for fluids.*, Wiley (1989).
- [16] R. KIMMEL AND J.A. SETHIAN, *Computing Geodesic Paths on Manifolds*, Proc. Nat. Acad. Sci. , 95 (1998), pp. 8431–8435.
- [17] J. SOKOŁOWSKI, A. ŻOCHOWSKI, *Topological derivatives of shape functionals for elasticity systems*. Mech. Structures Mach., **29**, no. 3, 331–349 (2001).
- [18] J. SOKOŁOWSKI J.-P. ZOLESIO, *Introduction to Shape Optimization : Shape Sensitivity Analysis*, Springer Ser. Comput. Math., vol. 10, Springer, Berlin (1992).
- [19] J. STRAIN, *Semi-Lagrangian Methods for Level Set Equations*, J. Comput. Phys., 151 (1999) pp. 498–533.
- [20] M.Y. WANG, X. WANG, D. GUO, *A level set method for structural topology optimization*, Comput. Methods Appl. Mech. Engrg., **192**, 227–246 (2003).